J. Fluid Mech. (1992), *vol.* 245, *pp.* 175–189

A note on the effects of viscosity on the stability of a trailing-line vortex

By PETER W. DUCK[1] AND MEHDI R. KHORRAMI[2]

[1] Department of Mathematics, University of Manchester, Manchester M13 9PL, UK

[2] High Technology Corporation, 28 Research Drive, Hampton, VA 23666, USA

(Received 23 September 1991)

The linear stability of the Batchelor (1964) vortex is investigated. Particular emphasis is placed on modes found recently in a numerical study by Khorrami (1991). These modes have a number of features very distinct from those found previously for this vortex, including (i) exhibiting small growth rates at large Reynolds numbers and (ii) susceptibility to destabilization by viscosity. In this paper these modes are described using asymptotic techniques, producing results which compare very favourably with fully numerical results at large Reynolds numbers.

1. Introduction

Stability analysis of streamwise vortices plays an important role in such diverse areas as wake-hazard reduction, combustor optimization, and three-dimensional separation control. Employing the Batchelor vortex (Batchelor 1964) for the mean velocity profile, a great deal of effort has been directed towards understanding the stability characteristics of a trailing-line vortex; the numerical works of Lessen, Singh & Paillet (1974), Lessen & Paillet (1974) and Duck & Foster (1980) should be mentioned. Using asymptotic analysis, the findings of the above authors were confirmed by many investigators, including Stewartson (1982), Leibovich & Stewartson (1983), Stewartson & Capell (1985), Stewartson & Brown (1985), Duck (1986), and Stewartson & Leibovich (1987). These asymptotic studies reveal the complex nature and structures of the inviscid modes with large negative azimuthal wavenumbers. Furthermore, they showed the intricacies and difficulties associated with the numerical computations of these instabilities. However, the extension of these results to the case of low azimuthal wavenumbers is of course not valid. Similar analyses based on inviscid disturbances with positive wavenumbers have failed to reveal any unstable modes. Indeed, most of the above studies treated only inviscid disturbances, with the possible exception of the work of Stewartson (1982), and viscosity is believed to have a stabilizing influence, generally.

Recently, using a numerical method, Khorrami (1991) found new viscous modes of instability for the Batchelor vortex. The two reported modes are for positive azimuthal wavenumbers which previously were thought to be stable. Furthermore, Khorrami found that these modes differed in two respects from the previously studied inviscid disturbances. First, they had no associated higher modes, and second they had growth rates which were generally orders of magnitude smaller. In the light of this, it seems quite unlikely that these new instabilities have structures similar to the inviscid perturbations reported by previous investigators. However, numerical methods are not the proper tool for providing either scale and structural information or a limiting analysis near the neutral curves for these modes. This paper

is an effort to address these concerns, as well as to provide firmer grounds for the existence of the instability modes with positive (and zero) azimuthal wavenumbers for the Batchelor vortex. A combination of asymptotic and numerical analysis is presented.

2. Problem formulation

If (u^*, v^*, w^*) denote the dimensional velocity components in the axial (x^*), radial (r^*), and azimuthal (θ) directions respectively, then the similarity solution of swirling wake flows at high Reynolds numbers due to Batchelor (1964) may be written

$$w_0^* = (C_0/r^*)(1-\mathrm{e}^{-\eta}), \tag{2.1}$$

$$u_0^* = U_0 - \frac{C_0 \mathrm{e}^{-\eta}}{8\nu x^*}\log\left(\frac{U_0 x^*}{\nu}\right) + \frac{C_0^2}{8\nu x^*}Q(\eta) - \frac{LU_0^2}{8\nu x^*}\mathrm{e}^{-\eta}, \tag{2.2}$$

where

$$\eta = U_0 r^{*2}/(4\nu x^*), \tag{2.3}$$

ν is the kinematic viscosity of the (incompressible) fluid, L is a constant (akin to a drag coefficient), C_0 is the circulation at large radius, and

$$Q(\eta) = \mathrm{e}^{-\eta}\{\log\eta + \mathrm{ei}(\eta) - 0.807\} + 2\mathrm{ei}(\eta) - 2\mathrm{ei}(2\eta), \tag{2.4}$$

where

$$\mathrm{ei}(\eta) = \int_\eta^\infty \frac{\mathrm{e}^{-\zeta}}{\zeta}\mathrm{d}\zeta. \tag{2.5}$$

Batchelor (1964) showed that the term involving $Q(\eta)$ in (2.2) was numerically much smaller in magnitude than the other terms, consequently it will be neglected in the present analysis. Similar assumptions were implemented by earlier studies on the stability of this class of vortical flow, as detailed in the previous section. Following Lessen *et al.* (1974), we scale velocity by

$$U_s = \frac{C_0^2}{8\nu x^*}\log\frac{U_0 x^*}{\nu} + \frac{LU_0^2}{8\nu x^*}, \tag{2.6}$$

and length by

$$r_s = (4\nu x^*/U_0)^{\frac{1}{2}}. \tag{2.7}$$

This leads to a non-dimensional mean-flow profile given by

$$U = (U_0/U_s) - \mathrm{e}^{-r^2}, \tag{2.8}$$

$$W = (q/r)(1-\mathrm{e}^{-r^2}), \tag{2.9}$$

where

$$q = C_0/(2\pi U_s r_s), \tag{2.10}$$

and

$$r = r^*/r_s = \eta^{\frac{1}{2}}. \tag{2.11}$$

We now write the velocity field as the sum of the mean flow together with a small-amplitude perturbation, namely

$$u^* = U_s(U+\delta\tilde{u}), \quad v^* = U_s\,\delta\tilde{v}, \quad w^* = U_s(W+\delta\tilde{w}), \tag{2.12}$$

while the pressure is written as

$$P^* = \rho U_0^2[\Pi + \delta\tilde{p}], \tag{2.13}$$

where

$$\Pi = (C_0^2 U_0/8\nu x^* U_s^2)\,Q_1(r), \tag{2.14}$$

with

$$Q_1(r) = (1-\mathrm{e}^{-r^2})/r + 2\mathrm{ei}(r^2) - 2\mathrm{ei}(2r^2). \tag{2.15}$$

A tilde quantity here represents the perturbation about the mean state and δ is the (small) perturbation amplitude. We now make the further assumption that U and W (and indeed also U_0) are independent of x^*. This will generally be an improper assumption, and is equivalent to a parallel-flow approximation (which has been used as an assumption in a number of diverse stability investigations). However, we justify this step on the following grounds. First, one of the primary aims of this paper is to develop asymptotic theories to compare with previous numerical results, which were all based on the same parallel-flow approximation. Second, since to leading order the solutions with which we are concerned turn out to be inviscid in form, it can be shown that to first order the parallel-flow approximation is a right and proper one.

We now return to consideration of the form to be taken for the perturbation quantities. We write

$$(\tilde{u},\tilde{v},\tilde{w},\tilde{p}) = \{F(r), \mathrm{i}G(r), H(r), P(r)\}\exp\{\mathrm{i}(\alpha x + n\theta - act)\}, \tag{2.16}$$

where α and n are the axial and azimuthal wavenumbers respectively, and $c = c_r + \mathrm{i}c_i$ is the complex wave speed. It turns out that the problem remains essentially unaltered if we use

$$U = \mathrm{e}^{-r^2} \tag{2.17}$$

as the mean axial velocity distribution. The net effect of this is solely on c_r, while the important amplification rate c_i is totally unaffected.

If we then substitute (2.12), (2.13), and (2.16) into the equations of motion, and consider terms of $O(\delta)$, we obtain

$$G' + G/r + \alpha F + nH/r = 0, \tag{2.18}$$

$$-\mathrm{i}\frac{G''}{Re} - \frac{\mathrm{i}G'}{Re\,r} + \left[\frac{\mathrm{i}}{Re}\left\{\frac{n^2+1}{r^2}+\alpha^2\right\} - \phi\right]G + \left[\frac{2\mathrm{i}n}{Re\,r^2} - \frac{2W}{r}\right]H + P' = 0, \tag{2.19}$$

$$-\frac{H''}{Re} - \frac{1}{Re\,r}H' + \left[\mathrm{i}\phi + \frac{1}{Re}\left\{\frac{n^2+1}{r^2}+\alpha^2\right\}\right]H + \left[\mathrm{i}\frac{\mathrm{d}W}{\mathrm{d}r} + \mathrm{i}\frac{W}{r} + \frac{2n}{Re\,r^2}\right]G + \mathrm{i}\frac{nP}{r} = 0, \tag{2.20}$$

$$-\frac{F''}{Re} - \frac{1}{Re\,r}F' + \left[\mathrm{i}\phi + \frac{1}{Re}\left\{\frac{n^2}{r^2}+\alpha^2\right\}\right]F + \mathrm{i}\frac{\mathrm{d}U}{\mathrm{d}r}G + \mathrm{i}\alpha P = 0, \tag{2.21}$$

where a prime denotes differentiation with respect to the radial coordinate. Here the Reynolds number is defined as

$$Re = U_s r_s/\nu, \tag{2.22}$$

and

$$\phi = \alpha(U-c) + nW/r. \tag{2.23}$$

The boundary conditions that must be imposed on this system are: at $r = 0$

$$\begin{aligned} &G(0) = H(0) = F'(0) = P'(0) = 0 && \text{for } n = 0,\\ &G'(0) = G(0) \pm H(0) = F(0) = P(0) = 0 && \text{for } n = \pm 1,\\ &F(0) = G(0) = H(0) = P(0) = 0 && \text{for } n > 1, \end{aligned} \tag{2.24}$$

while as $r \to \infty$,

$$F(r), G(r), H(r), P(r) \to 0. \tag{2.25}$$

In the following sections we study the above system in the limit as $Re \to \infty$.

3. The general leading-order behaviour as $Re \to \infty$

A number of papers previously addressed the inviscid limit of the system (2.18)–(2.21), (2.24), (2.25), in particular for modes which exhibit finite temporal growth rates (αc_i) in this limit. Rather than concern ourselves with these modes, we focus on another family of modes found numerically by Khorrami (1991). These exhibit significantly diminishing growth rates with a decrease in viscosity. Inspection of a number of these results, and others not reported, suggested the following two general characteristics of these modes as $Re \to \infty$: (i) $c_r = O(1)$ and (ii) $c_i = O(Re^{-1})$. These trends strongly suggest we seek an asymptotic expansion to our solution of the form

$$\{F, G, H, P\} = \{F_0, G_0, H_0, P_0\} + Re^{-1}\{F_1, G_1, H_1, P_1\} + O(Re^{-2}), \tag{3.1}$$

$$c = c_0 + Re^{-1}c_1 + O(Re^{-2}), \tag{3.2}$$

where we expect c_0 to be real. Here we are neglecting the effects of viscosity to leading order by assuming that the neutral modes will not be singular; this is strongly suggested by the viscous calculations of Khorrami (1991). Substituting (3.1), (3.2) into (2.18)–(2.21) and taking just $O(1)$ terms yields the following (inviscid) system of equations

$$G_0' + G_0/r + \alpha F_0 + nH_0/r = 0, \tag{3.3}$$

$$\phi_0 G_0 + 2WH_0/r = P_0', \tag{3.4}$$

$$\phi_0 F_0 + U'G_0 = -\alpha P_0, \tag{3.5}$$

$$\phi_0 H_0 + (W' + W/r)G_0 = -nP_0/r, \tag{3.6}$$

where

$$\phi_0 = \alpha(U - c_0) + nW/r. \tag{3.7}$$

Further, F_0 and H_0 may be eliminated between these equations to yield the following ordinary differential equations as determined by Duck & Foster (1980):

$$\frac{\mathrm{d}G_0}{\mathrm{d}r} = \left[\frac{n(rW)' + \alpha r^2 U'}{r^2\phi_0} - \frac{1}{r}\right]G_0 + \frac{n^2 + \alpha^2 r^2}{r^2\phi_0}P_0, \tag{3.8}$$

or symbolically

$$L_1\{G_0, P_0\} = 0, \tag{3.9}$$

together with

$$\frac{\mathrm{d}P_0}{\mathrm{d}r} = \left[\phi_0 - \frac{(W^2r^2)'}{r^3\phi_0}\right]G_0 - \frac{2nW}{r^2\phi_0}P_0, \tag{3.10}$$

or symbolically

$$L_2\{G_0, P_0\} = 0. \tag{3.11}$$

The boundary conditions may be simply inferred from (2.24) and (2.25).

Equations (3.8), (3.10) (and equivalent) have been investigated by a number of authors (e.g. Lessen *et al.* 1974; Duck & Foster 1980), in particular for complex values of the wave speed c_0. For this study, we carried out a similar investigation but sought real values of c_0.

A Chebyshev spectral collocation method was employed to perform the numerical tasks throughout this study, since spectral techniques are well known for their accuracy and fast convergence rate. The mathematical theory of such methods is found in Gottlieb & Orszag (1977) and Gottlieb, Hussaini & Orszag (1984, p. 1) and

is not presented here. Its implementation for the stability of swirling flows is given in detail by Khorrami, Malik & Ash (1989), and readers are referred to that paper for further information. Briefly, the method consists of expanding each perturbation eigenfunction in a truncated Chebyshev series, for example

$$G(\xi) = \sum_{k=0}^{N} a_k T_k(\xi), \tag{3.12}$$

where ξ is the independent variable in Chebyshev space. The governing equations (3.3) and (3.6), in discretized form, are then arranged in a generalized eigenvalue format. That is, if $\boldsymbol{D}$ and $\boldsymbol{E}$ represent the coefficient matrices, then

$$\boldsymbol{D}\bar{\boldsymbol{X}} = \omega \boldsymbol{E}\bar{\boldsymbol{X}}, \tag{3.13}$$

where the frequency $\omega = \alpha c$ is the eigenvalue, and the eigenvector $\bar{\boldsymbol{X}}$ is represented by

$$\bar{\boldsymbol{X}} = \{GHFP\}^{\mathrm{T}}. \tag{3.14}$$

It should be realized that $\boldsymbol{E}$ is a singular matrix. The singularity was removed by adding the term $\gamma\omega p$ (which is called an artificial compressibility factor) to the continuity equation (see Malik & Poll 1985), where γ is a small parameter of the order of 10^{-18}. This has been shown to have a negligible effect on the computed physical eigenvalues as reported by Khorrami *et al.* (1989). The method is global and therefore the entire eigenvalue spectrum could be obtained in a single run. The complex generalized eigenvalue solver employed was the IMSL QZ routine 'EIGZC'.

The outer boundary conditions were enforced at $r_{\max} = 100$, and the number of Chebyshev polynomials required varied depending on flow conditions, but usually was in the range between 60 and 80. At each step, care was taken to ensure that results were accurate to at least six or seven significant figures. The eigenfunctions were obtained using an inverse Rayleigh's method (see Wilkinson 1965). The discretization for the local scheme was also spectral. In fact, the same matrices $\boldsymbol{D}$ and $\boldsymbol{E}$ were used to compute the eigenfunctions.

It developed that the results from this study for $n = 0$ were somewhat different from those of $n \neq 0$; this has important implications on the asymptotic structure of the solution. Consequently, we shall consider the axisymmetric case separately.

4. Axisymmetric ($n = 0$) modes

For $n = 0$, our numerical scheme produced results for wave speed c_0 over a range of values of swirl parameter q and axial wavenumber α that had the following general features: (i) a number of *distinct*, *real* modes exist, (ii) all these modes have $c_0 < 0$, and (iii) these modes were quite distinct from those of other studies (e.g. Lessen *et al.* 1974; Duck & Foster 1980) for which $c_i \neq 0$. The present routine was able to generate these other modes, which served as a useful check on the accuracy of our scheme. Results for the variation of c_0 with α for the case $n = 0$, and $q = 1.0$, are presented in figure 1. Note that two distinct modes are shown. We believe these modes to be the two most important/dominant in this case. We refer to the mode represented by a solid line as mode I, and that represented by a broken line as mode II.

Note that the significance of $c_0 < 0$ is that no critical layers exist (i.e. $\phi_0 \neq 0$ for all r), a feature that leads to certain simplifications. The key question now is whether these modes are stable or unstable, since the study so far only reveals them to be neutrally stable in the limit of large Reynolds numbers. To determine the effects of

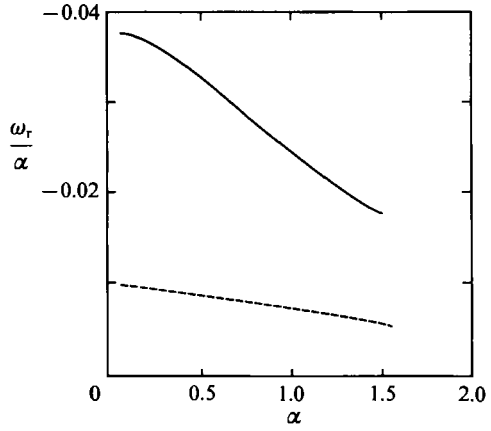

FIGURE 1. c_0 *vs.* α, $n = 0$, $q = 1.0$, inviscid calculations: ——, mode I; – – –, mode II.

viscosity on these modes, we must consider terms $O(Re^{-1})$ in (2.18)–(2.21). After some algebra, we obtain the following two first-order equations for G_1 and P_1:

$$L_1(G_1, P_1) = R_a, \tag{4.1}$$

$$L_2(G_1, P_1) = R_b. \tag{4.2}$$

We may write

$$R_a = R_{a_1} + \mathrm{i}c_1 R_{a_2}, \quad R_b = R_{b_1} + \mathrm{i}c_1 R_{b_2}, \tag{4.3}$$

where

$$R_{a_1} = -\frac{nR_3}{r\phi_0} - \frac{\alpha R_1}{\phi_0}, \quad R_{b_1} = -R_2 + \frac{2W}{r\phi_0} R_3, \tag{4.4}$$

$$R_{a_2} = -(\alpha/\phi_0)[nH_0/r + \alpha F_0], \tag{4.5}$$

$$R_{b_2} = -\alpha[G_0 - (2W/r\phi_0) H_0], \tag{4.6}$$

and

$$R_1 = -F_0'' - \frac{1}{r}F_0' + \left(\frac{n^2}{r^2} + \alpha^2\right)F_0, \tag{4.7}$$

$$R_2 = -G_0'' - \frac{1}{r}G_0' + \left[\frac{n^2+1}{r^2} + \alpha^2\right]G_0 + \frac{2n}{r^2}H_0, \tag{4.8}$$

$$R_3 = -H_0'' - \frac{1}{r}H_0' + \left[\frac{n^2+1}{r^2} + \alpha^2\right]H_0 + \frac{2n}{r^2}G_0. \tag{4.9}$$

Here we retain n since these equations are also useful for other values of n.

To solve the system of equations (4.1) and (4.2), we use standard theory relating to non-homogeneous linear ordinary differential equations (Ince 1956). According to this theory, in order that (4.1), and (4.2) have a solution, with boundary conditions given by (2.24), (2.25), certain solvability conditions must be met. For the present problem, we must have

$$c_1 = -\mathrm{i}\int_0^\infty [G^+ R_{a_1} + P^+ R_{b_1}]\,\mathrm{d}r \Big/ \int_0^\infty [G^+ R_{a_2} + P^+ R_{b_2}]\,\mathrm{d}r, \tag{4.10}$$

where G^+ and P^+ are the functions adjoint to the system (3.8), (3.10), i.e.

$$\frac{\mathrm{d}G^+}{\mathrm{d}r} = -\left[\frac{n(rW)' + \alpha r^2 U'}{r^2\phi_0} - \frac{1}{r}\right]G^+ - \left[\phi_0 - \frac{(W^2r^2)'}{r^3\phi_0}\right]P^+, \tag{4.11}$$

$$\frac{\mathrm{d}P^+}{\mathrm{d}r} = -\left[\frac{n^2 + \alpha^2 r^2}{r^2\phi_0}\right]G^+ + \frac{2nW}{r^2\phi_0}P^+, \tag{4.12}$$

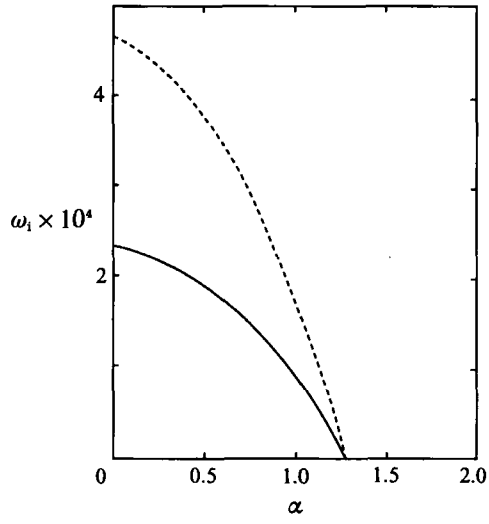

FIGURE 2. ω_i *vs.* α, $n = 0$, $q = 1.0$, asymptotic results, mode I: ——, $Re = 10000$; – – –, $Re = 5000$.

with boundary conditions

$$\begin{aligned} P^+(0) = G^{+\prime}(0) = 0 \quad &\text{if} \quad n = 0, \\ P^{+\prime}(0) = G^+(0) = 0 \quad &\text{if} \quad n = \pm 1, \\ P^+(0) = G^+(0) = 0 \quad &\text{if} \quad |n| > 1, \end{aligned} \tag{4.13}$$

and $P^+, G^+ \to 0$ as $r \to \infty$, for all n.

Note that owing to the nature of the solution for c_0 real, c_1 must be imaginary. The adjoint system (4.11) and (4.12) was discretized similarly to the case of the governing equations (3.3)–(3.6). However, owing to the nonlinear occurrence of ϕ_0 in (4.11) which results in a quadratic term for the frequency, ω, a slightly different approach was taken. Here, the eigenvalues were obtained using a companion matrix method. The method is very straight-forward (see Bridges & Morris 1984 and Khorrami *et al.* 1989), and involves linearizing the quadratic term by the following transformation:

$$\bar{P}^+ - \omega P^+ = 0, \tag{4.14}$$

which leads to a third equation for the adjoint set. For this case, the eigenvector $\bar{\boldsymbol{X}}$ in (3.13) then becomes

$$\bar{\boldsymbol{X}} = \{G^+ P^+ \bar{P}^+\}^{\mathrm{T}}. \tag{4.15}$$

It must be mentioned that for each computation, the computed eigenvalue spectrum of the adjoint system matched the spectrum associated with the original set, i.e. (3.3)–(3.6). This is an independent check on the accuracy and integrity of the results.

To obtain c_1, a Gauss–Chebyshev quadrature was employed to evaluate the integrals of (4.10); the procedure is straightforward. To ensure accurate results, the number of Chebyshev polynomials, N, was increased until c_1 had converged to at least five significant figures. Typically 90 to 100 polynomials were more than sufficient to obtain the required accuracy. Results for $\omega_i = \mathrm{Im}\{\alpha c_1/Re\}$ where $n = 0$, $q = 1.0$, $Re = 5000$ and 10000 are shown on figure 2 for mode I. It is clear that the first of these modes (figure 1) is destabilized over a range of α with the introduction of the effects of viscosity. Meanwhile, the results for ω_i for mode II are shown in figure

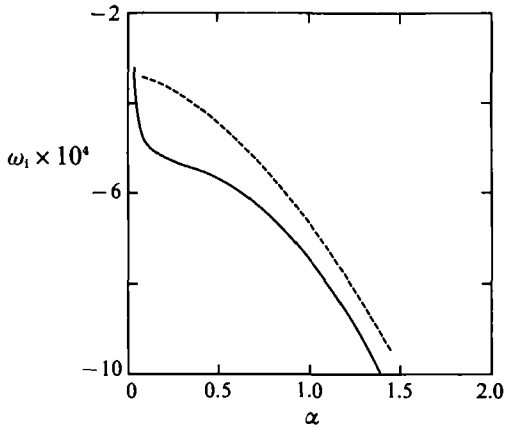

FIGURE 3. ω_i *vs.* α, $n = 0$, $q = 1.0$, $Re = 10000$, mode II: ——, fully viscous numerical; – – –, asymptotic.

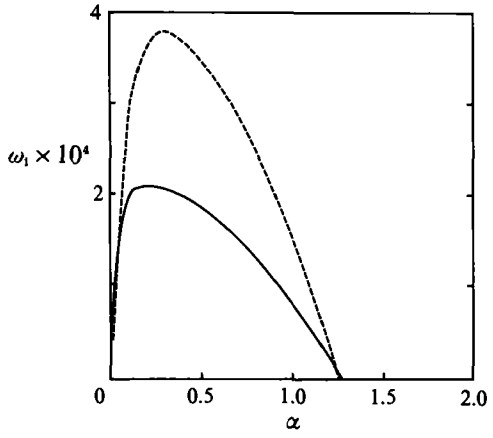

FIGURE 4. ω_i *vs.* α, $n = 0$, $q = 1.0$, fully viscous numerical results: ——, $Re = 10000$; – – –, $Re = 5000$.

3, and it is clear that viscosity stabilizes this mode. Also shown (on figure 4) are results for $\omega_i = \mathrm{Im}\{\alpha c_i\}$ for mode I obtained using the fully viscous routine of Khorrami (1991), at the same values of q and Reynolds number. The fully viscous results appear to exhibit an upper neutral point which is predicted extremely effectively by our asymptotic results. The growth rate αc_i in the region of the upper neutral point is also predicted accurately by asymptotic theory. However, there is an important point of disagreement concerning the nature of αc_i as $\alpha \to 0$ between the $Re \gg 1$ results and those for the full viscous equations. According to our asymptotic theory this quantity approaches a finite value as $\alpha \to 0$ while the fully viscous computation predicts a (sharp) drop off at small values of α.

However, this point of disagreement is quite clear. If $|\alpha c_1|$ approaches a constant value as $\alpha \to 0$, then $c_1 \approx O(1/\alpha)$ as $\alpha \to 0$, and hence a breakdown in the wave speed expansion (3.2) must occur. Additionally, if $n = 0$, it is also clear that as $\alpha \to 0$, $\phi \to 0$ (for bounded c) for all r. Specifically this breakdown must occur when $\alpha = O(Re^{-1})$, and hence we define a scaled axial wavenumber

$$\bar{\alpha} = Re\,\alpha = O(1). \tag{4.16}$$

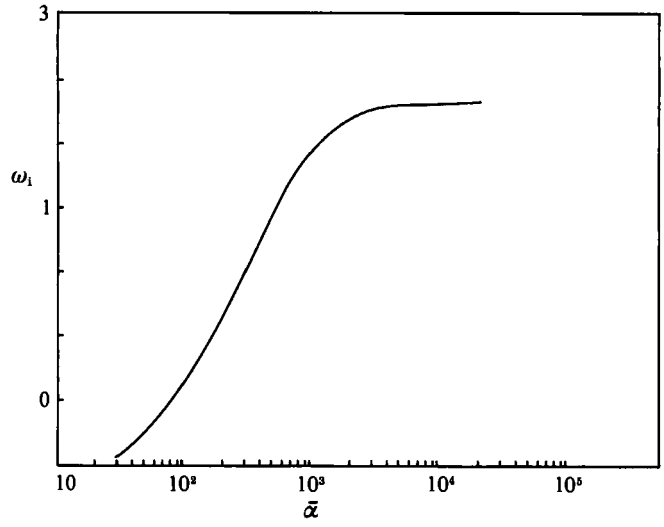

FIGURE 5. $\mathrm{Im}\{\bar{\alpha}c_0(\bar{\alpha})\}$ *vs.* $\bar{\alpha}$, $n = 0$, $q = 1.0$.

Guided by previous results for $\alpha \to 0$, and by consideration of the orders of magnitude of various terms in the governing equations, for $\bar{\alpha} = O(1)$ we must have

$$\left.\begin{aligned} F &= Re\hat{F}_0(r) + O(1), \quad G = \hat{G}_0(r) + O(Re^{-1}), \\ H &= Re\hat{H}_0(r) + O(1), \quad P = Re\hat{P}_0(r) + O(1), \end{aligned}\right\} \tag{4.17}$$

and the expansion for the complex wave speed (3.2) is retained. Substituting (4.17) into (2.18)–(2.21) and implementing (4.16), we obtain to leading order

$$\hat{G}_0' + \hat{G}_0/r + \bar{\alpha}\hat{F}_0 = 0, \tag{4.18}$$

$$2W\hat{H}_0/r = \hat{P}_0', \tag{4.19}$$

$$-\hat{H}_0'' - \frac{1}{r}\hat{H}_0' + \left[-\mathrm{i}\bar{\alpha}c_0 + \mathrm{i}\bar{\alpha}U + \frac{1}{r^2}\right]\hat{H}_0 + \left[\mathrm{i}\frac{\mathrm{d}W}{\mathrm{d}r} + \mathrm{i}\frac{W}{r}\right]\hat{G}_0 = 0, \tag{4.20}$$

$$-\hat{F}_0'' - \frac{1}{r}\hat{F}_0' + [-\mathrm{i}\bar{\alpha}c_0 + \mathrm{i}\bar{\alpha}U]\hat{H}_0 + \mathrm{i}\frac{\mathrm{d}U}{\mathrm{d}r}\hat{G}_0 + \mathrm{i}\alpha\hat{P}_0 = 0, \tag{4.21}$$

where the appropriate boundary conditions may be inferred from (2.24) and (2.25). The above system is then an eigenvalue problem for $c_0(\bar{\alpha})$, and was solved using a simplified form of the viscous routine used by Khorrami (1991). However, owing to the absence of the eigenvalue term in the r-momentum equation, matrix $\boldsymbol{E}$ becomes singular. Here the singularity is removed via a procedure which utilizes row and column operations (see Metcalfe & Orszag 1973). In this procedure, the rank of matrices $\boldsymbol{D}$ and $\boldsymbol{E}$ is reduced first and the eigenvalues are then obtained using the QZ routine. Results for $\mathrm{Im}\{\bar{\alpha}c_0(\bar{\alpha})\}$ are shown in figure 5 for the case $q = 1.0$, first mode. It is quite clear that a lower neutral point is predicted (at $\bar{\alpha} \approx 90$), while as $\bar{\alpha} \to \infty$, $\mathrm{Im}\{\bar{\alpha}c_0(\bar{\alpha})\} \to 2.3$. This is in agreement with the values shown on figure 2 as $\alpha \to 0$. Indeed a routine asymptotic analysis of the system (4.18)–(4.21) as $\bar{\alpha} \to \infty$ confirms a correct asymptotic match with the $\alpha = O(1)$, $\alpha \to 0$ solution.

The eigenfunctions near the upper neutral curve for the case of $n = 0$, $\alpha = 1.25$, $Re = 10000$ and $q = 1.0$ are shown in figure 6. The curves displayed were obtained

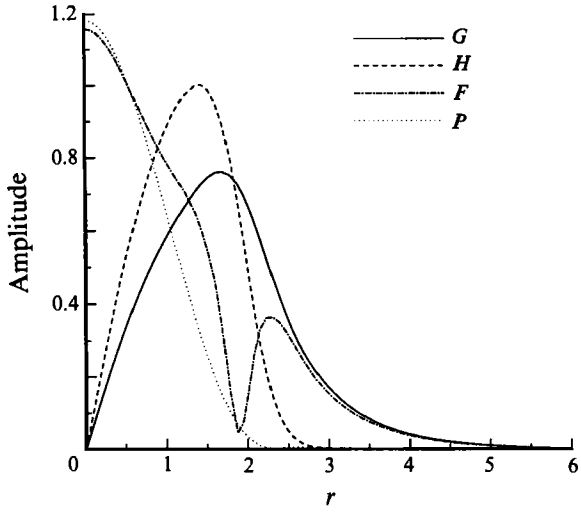

FIGURE 6. Eigenfunction components, $n = 0$, $\alpha = 1.25$, $Re = 10000$, $q = 1.0$, mode I, fully viscous calculations.

using the full viscous equations and are normalized with respect to the maximum value of the azimuthal component. Note that these viscous eigenfunctions are virtually indistinguishable from the inviscid eigenfunctions computed for the same parameters.

Thus, to summarize, we were able to predict (using two asymptotic analyses) both the upper and lower neutral points of this particular unstable mode as well as the temporal growth rates of the full viscous equation results (figure 4). Furthermore, the system (4.18)–(4.21) was also solved for the second (stable) mode, and it was found that this remained stable over the entire range of $\bar{\alpha}$. It should at this juncture be emphasized, however, that as $\alpha \to 0$, the use of the parallel-flow approximation is likely to become increasingly questionable.

In the following section we go on to consider the $n \neq 0$ modes, paying particular attention to cases for which $n = 1$; although there are some similarities with the axisymmetric case, some important and interesting differences also exist.

5. Non-axisymmetric modes

Khorrami (1991) presents results for an unstable mode (with a growth rate that diminishes as $Re \to \infty$) for the particular case $n = 1$. In this section we discuss the stability of such an asymmetric disturbance.

We initially follow the same approach as that carried out in the previous sections and apply these methods to the case $n = 1$, $q = 0.7$. Figure 7 shows the variation of c_0 (which again is real) with α, obtained from the solution of (3.3)–(3.6). Based on our numerical computations, this mode turned out to be similar to the slow bending mode obtained previously by Leibovich, Brown & Patel (1986). It displays the characteristic behaviour that both the frequency $\omega_r \to 0$ and the axial phase speed $c = \omega_r/\alpha \to 0$ as $\alpha \to 0$. The asymptotic results of Leibovich *et al.* (1986) evaluated for our mean velocity profile, are also plotted in figure 7. The asymptotic curve displays the correct trend and the agreement for small values of α is good.

Note that in figure 7, below a critical value of $\alpha (= \alpha_0$, say), we see $c_0 < 0$, while above this value c_0 becomes positive. We were able to continue the computation of

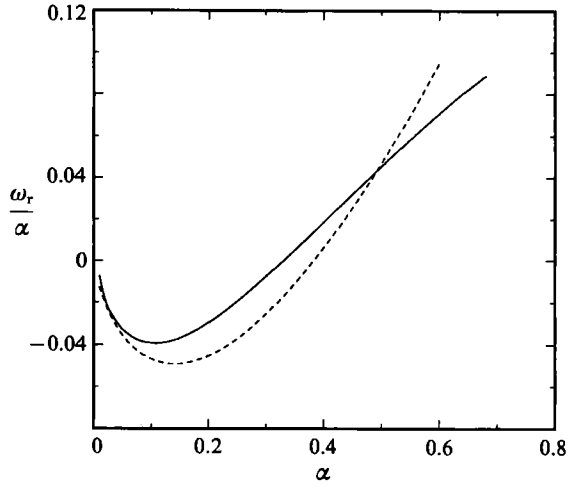

FIGURE 7. c_0 *vs.* α, $n = 1$, $q = 0.7$; ——, inviscid calculations: – – –, asymptotic results due to Leibovich *et al.* (1986).

c_0 beyond α_0 using the numerical scheme described in §3. However, since $c_0 > 0$, and our numerical results suggested c_0 remained real, a critical layer must be present at any point, r_0, at which $\phi_0 = 0$. Hence computation of such modes, according to Lin (1955), must be carried out by extending the computation into complex r-space to avoid the singularity in the differential equation. Although our numerical scheme performed extremely well, by its nature it is not amenable for obtaining solutions off the real r-axis. (The authors did attempt a Runge–Kutta scheme for treating (3.3)–(3.6), but extremely small grid sizes, which required prohibitively longer computer times, were necessary for adequate resolution of these modes. This was found even for examples in which $c_0 < 0$, i.e. for which no critical layer existed. Further, many spurious modes were generated with this technique.) However, below we suggest why it may be possible to extend these computations of (3.3)–(3.6) a little way into regimes where critical layers may exist, without any special modification of the scheme, or numerical difficulties.

Let us initially confine our attention to values of $\alpha < \alpha_0$, for which the techniques and analysis of the previous section are applicable without modification. In particular, the computed values of ω_i obtained from (4.10) are shown in figure 8 as points denoted by circles for the case $n = 1$, $q = 0.7$. They are to be compared with the values of ω_i obtained using the full viscous equations for the same case, at $Re =$ 6000 and 10000, as presented in the same figure. The computed and asymptotic values proved to be indistinguishable on the scale shown in figure 8. It is apparent that we are able to predict, using our asymptotic theory, the location of the lower neutral point (at $\alpha \approx 0.05$) without the requirement of a further $\alpha \ll 1$ substructure. Agreement between the asymptotic and fully numerical results was excellent up to $\alpha = \alpha_0$, the point to which our asymptotic results extend. However, once $\alpha > \alpha_0$, the critical layer situated at r_0 moves into the computational domain. Analysis of (3.3)–(3.6) revealed that the inviscid solutions are almost regular if the critical layer is sufficiently far away from the centreline of the vortex. From the physical point of view, this means that the critical layer should remain in the potential region of the vortex (see analysis below). The numerical results confirmed that for most values of α (except very close to the upper neutral curve) r_0 remained large. Our inability to

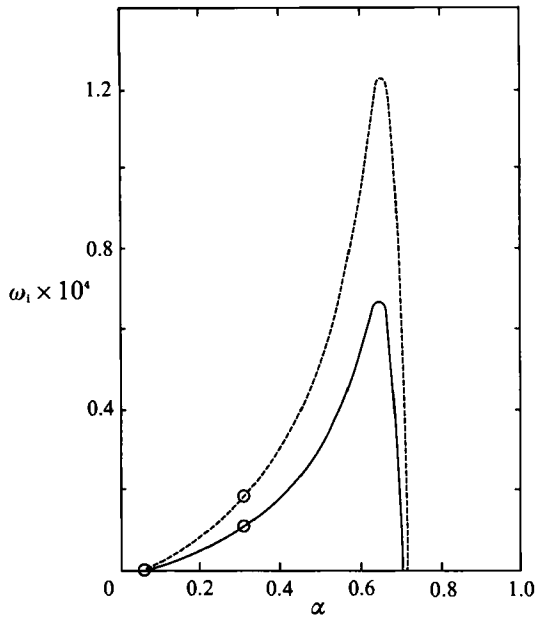

FIGURE 8. ω_i *vs.* α, $n = 1$, $q = 0.7$, fully numerical results (circles denote asymptotic points): ——, $Re = 10000$; – – –, $Re = 6000$.

obtain the viscous corrections, (4.10), is mainly due to the failure of the local and global methods to converge while computing the adjoint system. Here, the singularity plays a more dominant role.

As α becomes greater than α_0, the full viscous equations yield values of ω_i which initially continue to increase but then rapidly drop in value to give an upper neutral point. In some ways the drop for the lower Reynolds number can appear more dramatic, but this is simply explained by the fact that the values of ω_i decrease with an increase in Reynolds number.

For $\alpha > \alpha_0$, it appears that there are two distinct possibilities to explain this behaviour. The first possibility, if c_0 remains real, implies that a critical layer exists on the real axis and hence a singular solution in general, although it is possible to show that the coefficient of this singularity is asymptotically small as $r_0 \to \infty$ on account of the base flow (i.e. this occurs as a result of the previously neglected exponentially small terms). This could explain why the singular component of the solution is not readily observed, and perhaps why we were able to extend our numerical scheme for the system (3.3)–(3.6) beyond $\alpha = \alpha_0$ without any special modification or difficulties.

However, as α increases, r_0 moves towards the centre of the vortex ($r = 0$). If c_0 remains real, ultimately the presence of a critical layer will become important, in particular its effect will be profound when $r_0 = O(1)$, implying $\alpha - \alpha_0 = O(1)$. Perhaps it is this penetration of the critical layer close to the vortex centre that triggers the sharp drop in growth rate αc_i with α, to yield the upper neutral point as seen in the fully viscous solutions in figure 8. However, the presence of the critical layer requires that a detour be made into the complex r-plane when considering the inviscid equations. According to Lessen *et al.* (1974) this detour is below the real axis if $\mathrm{Re}\{\phi'(r_0)\} > 0$, and vice versa. As remarked earlier, our numerical scheme is confined to the real axis, and so we were unable to carry out the computations for our asymptotic structure beyond $\alpha = \alpha_0$ with any degree of certainty.

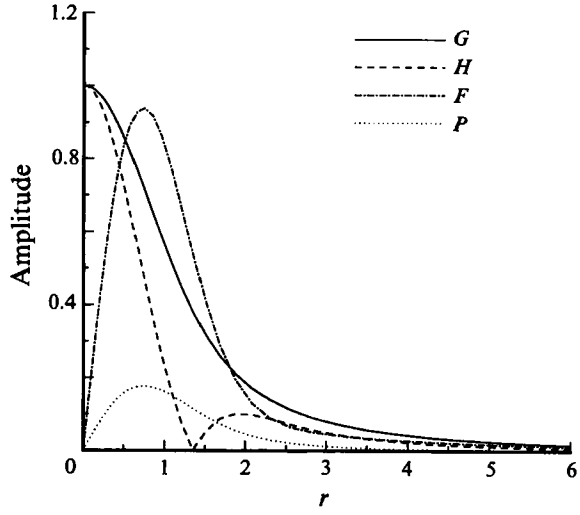

FIGURE 9. Eigenfunction components, $n = 1$, $\alpha = 0.3$, $q = 0.7$, inviscid calculations.

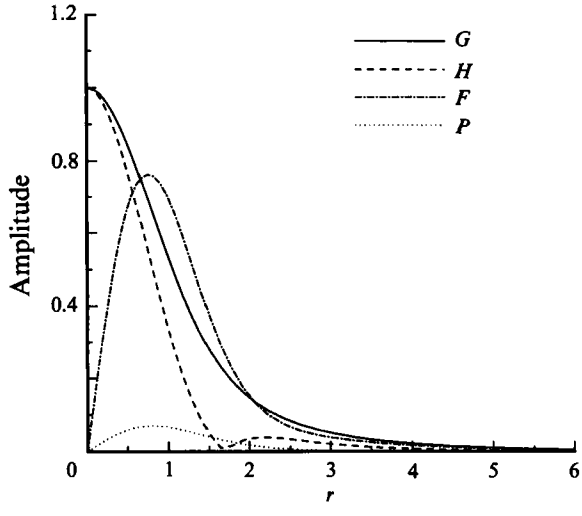

FIGURE 10. Eigenfunction components, $n = 1$, $\alpha = 0.6$, $q = 0.7$, inviscid calculations.

A second possibility exists, namely that the inviscid solution of (3.3)–(3.6) yields complex stable values of c_0 for $\alpha > \alpha_0$. This stable inviscid decay rate would then counteract the unstable viscous growth rate which could result in a rapid stabilizing trend for $\alpha > \alpha_0$. Note that although a computation of the inviscid system may yield two non-neutral values of c (one being the complex conjugate of the other), only one of these can be correct in the $Re \gg 1$ limit of the full viscous equations. The detour described above serves to select the appropriate root (Lin 1945*a–c*). Similar solutions are to be found in the stability of boundary layers (see Mack 1987).

In figures 9 and 10 the inviscid eigenfunctions (normalized by $H_{\max}$) for the case of $n = 1$ and $q = 0.7$ are presented. The results in figure 9 correspond to $\alpha = 0.3$ which is slightly below the critical value of the axial wavenumber, $\alpha_0 \approx 0.33$. The displayed eigenfunctions in figure 10 correspond to $\alpha = 0.6$ with the critical layer residing at $r \approx 4.1$. Comparing the two figures, there are hardly any noticeable differences. In

fact, the structure of this mode remains little changed through the upper neutral curve. Although not shown, the viscous eigenfunctions are virtually indistinguishable from the displayed curves in figures 9 and 10.

Certainly these eigensolutions show scanty evidence of a critical layer. But this should not be taken as disproving our first conjecture above, on account of the exponentially small coefficient of the singularity, as pointed out previously. Our numerical scheme was unable to give a categorical vindication of either of the two possibilities.

6. Conclusion

In this paper we have presented asymptotic analyses which describe and indeed conform the additional modes of instability due to viscosity recently found numerically for the trailing-line vortex by Khorrami (1991). Unlike the previously reported inviscid modes of instability, these modes are inviscidly neutral but are destabilized by viscosity.

Although our investigation has been confined exclusively to the trailing-line vortex, there is no reason why such mechanisms should not operate in the same way for other vortex flows.

Finally, it must be emphasized again that the parallel-flow approximation has been employed throughout this paper, and an interesting extension of this work would be to include the effects of non-parallelism.

The authors are grateful for the helpful comments of the referees. The work of P.W.D. was supported by the National Aeronautics and Space Administration under NASA Contract NAS1-18605 while P.W.D. was in residence at the Institute for Computer Science Applications in Science and Engineering, NASA Langley Research Center, Hampton, VA, 23665, USA. The work of M.R.K. was supported by NASA Langley Research Center (Experimental Flow Physics Branch) under NASA Contract NAS1-18240.

REFERENCES

Batchelor, G. K. 1964 Axial flow in the trailing line vortices. *J. Fluid Mech.* **20**, 645.

Bridges, T. J. & Morris, P. J. 1984 Differential eigenvalue problems in which the parameter appears nonlinearly. *J. Comput. Phys.* **55**, 437.

Duck, P. W. 1986 The inviscid stability of swirling flows: Large wavenumber disturbances. *Z. Angew. Math. Phys.* **37**, 340.

Duck, P. W. & Foster, M. R. 1980 The inviscid stability of a trailing line vortex. *Z. Angew. Math. Phys.* **31**, 523.

Gottlieb, D., Hussaini, M. Y. & Orszag, S. A. 1984 *Spectral Methods for Partial Differential Equations*. SIAM.

Gottlieb, D. & Orszag, S. A. 1977 *Numerical Analysis of Spectral Methods: Theory and Applications*. SIAM.

Ince, E. L. 1956 *Ordinary Differential Equations*. Dover.

Khorrami, M. R. 1991 On the viscous modes of instability of a trailing line vortex. *J. Fluid Mech.* **225**, 197.

Khorrami, M. R., Malik, M. R. & Ash, R. L. 1989 Application of spectral collocation techniques to the stability of swirling flow. *J. Comput. Phys.* **81**, 206.

Leibovich, S., Brown, S. N. & Patel, Y. 1986 Bending waves on inviscid columnar vortices. *J. Fluid Mech.* **173**, 595.

LEIBOVICH, S. & STEWARTSON, K. 1983 A sufficient condition for the instability of columnar vortices. *J. Fluid Mech.* **126**, 335.

LESSEN, M. & PAILLET, F. 1974 The stability of a trailing line vortex. Part 2. Viscous theory. *J. Fluid Mech.* **63**, 769.

LESSEN, M., SINGH, P. J. & PAILLET, F. 1974 The stability of a trailing line vortex. Part 1. Inviscid theory. *J. Fluid Mech.* **63**, 753.

LIN, C. C. 1945*a* On the stability of two-dimensional parallel flows. Part I. General theory. *Q. Appl. Maths* **3**, 117.

LIN, C. C. 1945*b* On the stability of two-dimensional parallel flows. Part II. Stability in an inviscid fluid. *Q. Appl. Maths* **3**, 218.

LIN, C. C. 1945*c* On the stability of two-dimensional parallel flows. Part III. Stability in a viscous fluid. *Q. Appl. Maths* **3**, 277.

LIN, C. C. 1955 *The Theory of Hydrodynamic Stability*. Cambridge University Press.

MACK, L. M. 1987 Review of linear compressible stability theory. *ICASE Workshop on the Stability of Time Dependent and Spatially Varying Flows*. Springer.

MALIK, M. R. & POLL, D. I. A. 1985 Effect of curvature on three-dimensional boundary layer stability. *AIAA J.* **27**, 1362.

METCALFE, R. W. & ORSZAG, S. A. 1973 Numerical calculation of the linear stability of pipe flows. *Flow Research Rep.* 25, *Contract* N00014-72-C-0365.

STEWARTSON, K. 1982 The stability of swirling flows at large Reynolds number when subjected to disturbances with large azimuthal wavenumber. *Phys. Fluids* **25**, 1953.

STEWARTSON, K. & BROWN, S. N. 1985 Near-neutral center-modes as inviscid perturbations to a trailing line vortex. *J. Fluid Mech.* **156**, 387.

STEWARTSON, K. & CAPELL, K. 1985 On the stability of ring modes in a trailing line vortex: the upper neutral point. *J. Fluid Mech.* **156**, 369.

STEWARTSON, K. & LEIBOVICH, S. 1987 On the stability of a columnar vortex to disturbances with large azimuthal wavenumber: the lower neutral points. *J. Fluid Mech.* **178**, 549.

WILKINSON, J. H. 1965 *The Algebraic Eigenvalue Problem*. Oxford University Press.